Pair Correlations and Photoassociation Dynamics of Two Atoms in an Optical Tweezer

M. Weyland,[1,2] S. S. Szigeti,[3] R. A. B. Hobbs,[1,2] P. Ruksasakchai,[1,2] L. Sanchez,[1,2] and M. F. Andersen[1,2,*]
[1]The Dodd-Walls Centre for Photonic and Quantum Technologies, University of Otago, Dunedin 9056, New Zealand
[2]Department of Physics, University of Otago, Dunedin 9054, New Zealand
[3]Department of Quantum Science, Research School of Physics, The Australian National University, Canberra 2601, Australia

(Received 31 August 2020; accepted 29 January 2021; published 25 February 2021)

We investigate the photoassociation dynamics of exactly two laser-cooled ^{85}Rb atoms in an optical tweezer and reveal fundamentally different behavior to photoassociation in many-atom ensembles. We observe nonexponential decay in our two-atom experiment that cannot be described by a single rate coefficient and find its origin in our system's pair correlation. This is in stark contrast to many-atom photoassociation dynamics, which are governed by decay with a single rate coefficient. We also investigate photoassociation in a three-atom system, thereby probing the transition from two-atom dynamics to many-atom dynamics. Our experiments reveal additional reaction dynamics that are only accessible through the control of single atoms and suggest photoassociation could measure pair correlations in few-atom systems. It further showcases our complete control over the quantum state of individual atoms and molecules, which provides information unobtainable from many-atom experiments.

DOI: 10.1103/PhysRevLett.126.083401

Chemical processes govern the natural world and are used to create desired molecular structures. Such reactions usually occur in macroscopic samples of atoms and molecules that interact in many different ways. However, the tantalizing prospect of assembling individual molecules atom by atom via optical tweezers is emerging [1–4]. Developed to its full capacity, this bottom-up approach could realize the enduring scientific ambition of arranging atoms in molecules the way we want [5–7]. Furthermore, studying the formation of individual molecules isolates the reaction dynamics of interest from additional undesirable processes, such as spurious intermolecular collisions, thereby giving unprecedented insight into the underlying physics.

An ideal process for controlled molecular formation is photoassociation, where light converts two colliding atoms into a molecule. Recent experiments have shown the formation of a single molecule via photoassociation [2,3] and magnetoassociation [4] of exactly two atoms. However, there has only been one prior study into the dynamics when photoassociating exactly two atoms [8], and its use of near-resonant light resulted in strong photon scattering, which made the atomic dynamics between collisions effectively classical.

Quantum correlations can change the photoassociation rate in many-atom systems [9]. Moreover, theoretical studies show that the photoassociation process itself can affect atom-atom correlations, leading to complex dynamics [10–13]. However, to date all experimental studies of photoassociation dynamics are well described by a single time-independent rate coefficient, indicating that photoassociation did not affect atom-atom correlations [14–19].

In this work, we observe the quantum dynamics of exactly two atoms undergoing photoassociation in an optical tweezer. The dynamics differs profoundly from those observed in many-atom ensembles. In particular, the dynamics is more complex and molecule formation cannot be described by a single rate coefficient. This is due to the pair correlation in the two-atom system; for two atoms the center-of-mass and relative-position degrees of freedom are separable in an optical tweezer. Consequently, thermally populated relative-position states either possess strongly positive pair correlations (with a high chance of finding the two atoms close together) or a node in the pair correlation function at zero interatomic separation (i.e., the atoms are anticorrelated and there is a low chance of finding the pair close together). Anticorrelated states are unaffected by photoassociation on short timescales, whereas relative-position eigenstates with strongly positive pair correlations lead to fast molecule formation. We confirm that this is the underlying cause by investigating the photoassociation dynamics of three atoms, which approach the well-known dynamics of many-atom experiments.

Experiment.—We prepare a single ^{85}Rb atom in an optical tweezer with an efficiency of around 80% and detect it using an EMCCD camera [20]. The single atoms are optically pumped into $|F = 2, m = -2\rangle$ in a 8.7 G magnetic quantization field. By adiabatically merging two spatially separated tweezers that each contain a single atom, we obtain one tweezer with exactly two atoms at a peak density of 1.7×10^{13} cm^{-3} [21]. Figure 1(a) shows the central components of the setup. We use a high-numerical aperture lens (NA = 0.55) to create the tightly focused light of the optical tweezers (red beams), as well as to

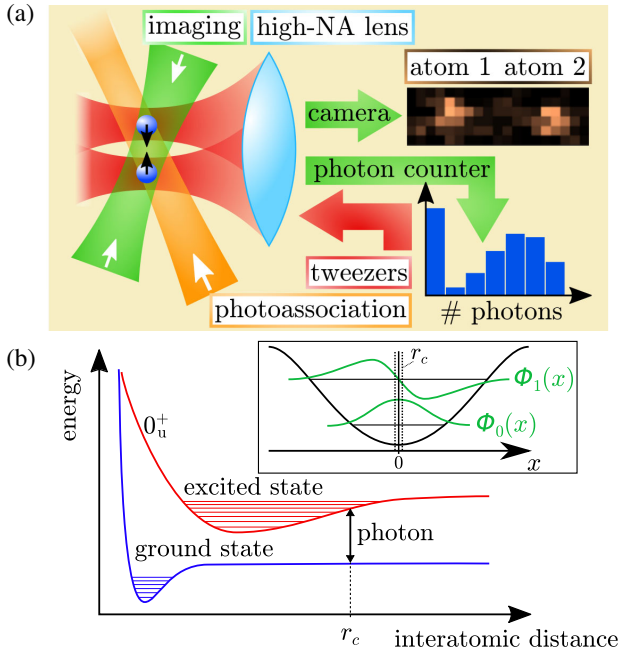

FIG. 1. (a) Schematic of experimental setup and measurement. Tweezer light is focused by a high-NA lens (NA = 0.55) to a radial diameter of 1.1 μm. Atoms in the tweezers are imaged using an EMCCD camera and merged into a single optical tweezer (black arrows). After applying photoassociation light, a single photon counter measures the population of the tweezer. Green and orange beams show imaging and photoassociation light, respectively. (b) Sketch of the photoassociation process. Inset: 1D slice of the two lowest energy relative-position eigenstates of two atoms in our optical tweezer, with Condon radius r_c marked for comparison.

collect a large proportion of the scattered imaging light (green beam), which is sent to the camera to confirm atom capture in both tweezers.

After transferring both atoms to the same tweezer, the atoms are exposed to photoassociation light at a frequency near 377.001 14 THz, 106 GHz red detuned from the atomic $D1$ transition. Using a stable cavity we can reproduce this frequency with a precision of 2 MHz. A Ti:sapphire laser delivers this light in 140 ns–duration pulses, during which the optical tweezer is turned off to eliminate any light shifts from the tweezer. Photoassociation dynamics occur on timescales from several microseconds to several milliseconds. We form molecules in a high vibrational level of a 0_u^+ state [Fig. 1(b)], with the target state determined by the polarization and frequency of the photoassociation light [19,22–25].

We detect a photoassociation event by imaging the tweezer after a given time of exposure to photoassociation light. Formed molecules either quickly decay to the ground state, which does not scatter imaging light, or back into two atoms, which have now received enough energy to escape the trap. In both cases no atoms remain in the tweezer. We use a single photon counter to precisely measure the amount of scattered imaging light, which allows us to determine the number of atoms in a single tweezer [26].

Pair correlation for two atoms.—Since the optical tweezer is well approximated as a harmonic potential, the two-atom center-of-mass and relative-motional degrees of freedom are separable. Our experiments are performed with identical bosonic ^{85}Rb atoms, so the even-parity eigenstates

$$\phi_{\mathbf{n}}(\mathbf{r}) = \varphi_{n_x}(x)\varphi_{n_y}(y)\varphi_{n_z}(z) \tag{1}$$

of the Hamiltonian

$$H_{\mathrm{rel}}(\mathbf{r}) = -\frac{\hbar^2}{2\mu}\nabla_{\mathbf{r}}^2 + \sum_{i=x,y,z}\frac{1}{2}\mu\omega_i^2 r_i^2 \tag{2}$$

form a complete set for the dynamics. Here, $\mathbf{r} = (x, y, z)$ is the relative-position coordinate and $\varphi_{n_i}(r_i)$ are eigenstates of a 1D harmonic oscillator with frequency ω_i and mass $\mu = m_{\mathrm{Rb}}/2$, with m_{Rb} the mass of a rubidium atom [Fig. 1(b) inset]. To ensure that $\phi_{\mathbf{n}}(\mathbf{r})$ is symmetric under particle exchange, $(-1)^{n_x+n_y+n_z} = 1$. At zero separation between the atoms, these eigenstates either have a peak (n_x, n_y, n_z all even) or a node (two of n_x, n_y, n_z odd, one even). Atom pairs thermally populate these relative-position eigenstates. Although including a finite-range atom-atom interaction modifies the eigenstates, the reflection symmetries of $H_{\mathrm{rel}}(\mathbf{r})$ persist for a spherically symmetric interaction. Therefore, the classification of two-atom states into strongly positive pair correlated (peaked) and anticorrelated (nodal) remains valid even in the presence of realistic interactions.

The pair correlations of the two-atom wave function strongly determine the photoassociation dynamics [10,27]. The strength of the photoassociation process depends on the wave function at the Condon radius r_c, the interatomic distance at which photoassociation light can resonantly transfer atoms to an electronically excited molecular potential [22]. In our experiment, $r_c = 4.3$ nm [24]. For laser-cooled atoms, the thermal de Broglie wavelength λ_{dB} is large compared to r_c, so the wave function at the Condon radius is either close to zero for anticorrelated nodal states or close to a maximum for strongly positive pair-correlated peaked states [Fig. 1(b) inset]. Consequently, atom pairs initially prepared in peaked eigenstates exhibit a much faster photoassociation rate compared to atom pairs initially prepared in nodal states. Therefore, photoassociation in the two-atom system requires at least a two-timescale model that accounts for the formation of molecules at two different rates. Contrast this to the many-atom case, which is described by a one-timescale model [15].

Two-timescale model of photoassociation.—Figure 2(a) shows a typical measurement of the probability of finding zero or two atoms in the optical tweezer as a function of photoassociation time. Red crosses show the probability

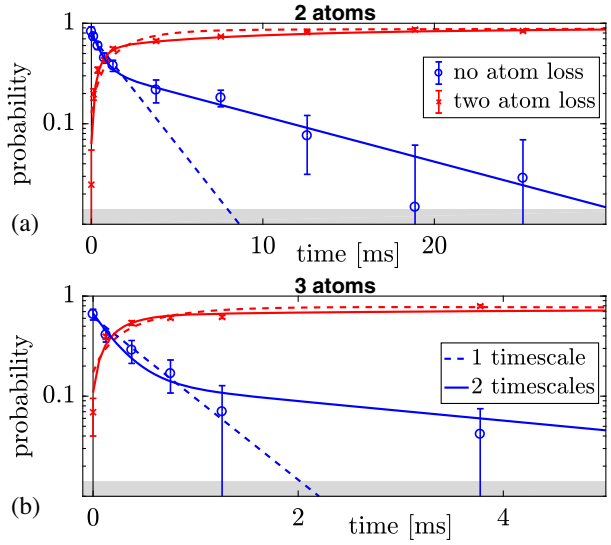

FIG. 2. Evolution of the tweezer's population as a function of photoassociation time for two atoms (a) and three atoms (b) at 35 μK. Given the measured radial and axial trapping frequencies of 88 and 14 kHz, respectively, this temperature corresponds to mean relative-motional mode occupations of $\bar{n}_r \sim 7$ in the radial directions and $\bar{n}_z \sim 40$ in the axial direction. In both panels, dashed and solid lines indicate the best one- and two-timescale fits to the experimental data, respectively. The gray area marks our detection sensitivity limit. Since the three-atom system has three atom pairs, compared to one in the two-atom system, we expect a decay timescale three times faster for the same rate coefficient.

that both atoms are lost due to photoassociation, while blue circles indicate the probability that both atoms remain. The one-timescale fit (dashed line) shows that the photoassociation dynamics cannot be reproduced using only one photoassociation rate. However, we obtain a good reproduction of the observed dynamics with a two-timescale model (solid line) that fits two independent two-atom populations with separate photoassociation rates [28].

Using a χ^2 test [29] on all rate measurements, we find that the one-timescale model is clearly rejected, while the two-timescale model is accepted in most cases [28]. Our statistical analysis shows the importance of atom-pair correlations on the photoassociation dynamics.

Further evidence for our two-timescale model is provided via a numerical simulation of the relative coordinate wave function $\psi(\mathbf{r}, t)$. Since photoassociation principally occurs near the Condon radius r_c [22], we use a simplified model that treats photoassociation as an absorbing hard-shell potential of strength $\hbar\Gamma$ and width w, located at relative distance r_c [28]:

$$i\hbar \frac{\partial}{\partial t}\psi(\mathbf{r}, t) = [H_{\mathrm{rel}}(\mathbf{r}) - iV_{\mathrm{PA}}(\mathbf{r})]\psi(\mathbf{r}, t), \tag{3}$$

where

$$V_{\mathrm{PA}}(\mathbf{r}) = \begin{cases} \hbar\Gamma, & r_c - w \le |\mathbf{r}| \le r_c, \\ 0, & \text{otherwise.} \end{cases} \tag{4}$$

We use $w = 0.38$ pm, corresponding to the interatomic distances accessible at the observed 28 MHz resonance width. Simulations are conducted by averaging over a thermal ensemble of initial states evolved under Eq. (3). The initial states are relative-position eigenstates $\phi_{\mathbf{n}}(\mathbf{r})$ of Eq. (2).

Our simulations qualitatively capture the two-timescale behavior seen in the experiment. As shown in Fig. 3(a), the fast timescale dynamics are primarily due to the decay of peaked states, whereas the decay of nodal states occurs on a slower timescale (see inset). Figure 3(b) shows the density of the thermal ensemble after applying different durations of photoassociation. The peak at zero atom-atom separation in the $t = 0$ plot is due to the bosonic enhancement of correlations in a thermal cloud. We observe a fast depletion of the density around zero atom-atom separation when evolving via Eq. (3), with the resultant density dip indicating that there is a low probability of both atoms being found at the same position. This rapid transition from a positively pair-correlated ensemble to an anticorrelated ensemble is reflected by the population dynamics [Fig. 3(a)], confirming that states peaked at $\mathbf{r} = 0$ photoassociate fast, while nodal states remain. As the system approaches the single-state limit applicable to ground-state-cooled tweezer experiments [34], the population of nodal states approaches zero and our simulations predict that photoassociation is dominated by the ground state dynamics and follows a fast decay.

The photoassociation of nodal states is considerably slower in the simulation than in the experiment. A significant contribution to this discrepancy is the lower simulation temperature [35]. Increasing the temperature rapidly increases the slow-decay rate relative to the fast-decay rate and furthermore increases the fraction of nodal (slow decaying) states [28]. Increasing the Condon radius also increases the slow rate relative to the fast rate [28]. The overall agreement between simulated and experimental timescales might also be improved with a different choice of Γ. Regarding the experiment, we have confirmed that population is not redistributed from nodal to peaked states while the atoms are held in the chopped tweezer [28]. However, any technical imperfection that breaks the reflection symmetry of the tweezer may increase the rate of the slow-decaying states in the experiment.

The experiments also show a higher proportion of fast-decaying states than the simulation. Again, the difference in temperature can contribute to this, since highly excited nodal states can also decay fast. Additionally, our preparation mechanism might not create a thermal equilibrium distribution. Finally, atom-atom interactions change the proportion of peaked to nodal states, although an estimate

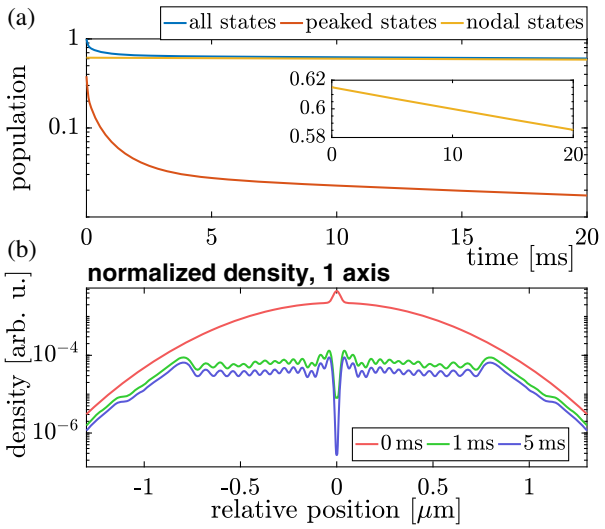

FIG. 3. Numerical simulation of the atom-pair evolution in the tweezer under photoassociation. (a) Population over time for an ensemble at 10.5 μK; also shown are the separate contributions due to states where n_x, n_y, n_z are all even (peaked states) and states where two of n_x, n_y, n_z are odd (nodal states). The inset shows the slow decay of nodal states. (b) 1D slice of the thermal ensemble density along the weak-trapping axis of the tweezer at different times since illumination with photoassociation light started. Simulations used trapping frequencies $(\omega_x, \omega_y, \omega_z) = 2\pi \times (93.0, 93.93, 20.0)$ kHz, consistent with our experimental setup, and $\Gamma = 2.802$ THz.

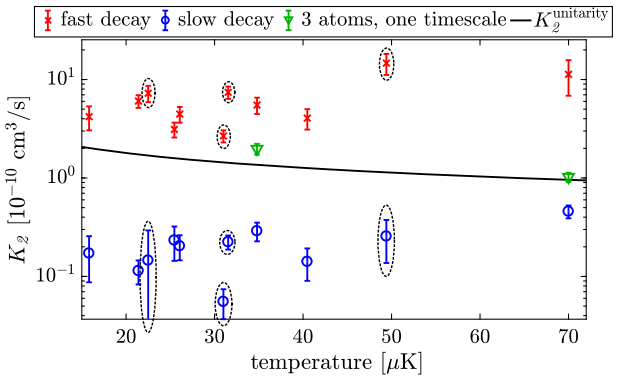

FIG. 4. Photoassociation rate coefficients with exactly two atoms in the optical tweezer for fast-decaying populations (ascribed primarily to peaked states) and slow-decaying populations (ascribed to nodal states), compared to the unitarity-limited rate coefficient [Eq. (5)]. Points in dashed circles show data at a light intensity of 230 W cm^{-2} with other points corresponding to 580 W cm^{-2}. Green triangles show the one-timescale rate coefficient in an optical tweezer with three atoms. The mean mode occupations of these experiments range from $\bar{n}_r \sim 4$–20 for the radial trapping directions and $\bar{n}_z \sim 30$–100 for the axial trapping direction.

of the ground state energy shift indicates that this effect is small.

Rate coefficients.—In many-atom ensembles, the single rate coefficient K_2 governing the photoassociation dynamics reaches its highest, unitarity-limited value for photoassociation light at the saturation intensity [7,17,30]. For photoassociation of two indistinguishable particles with a maximum photoassociation cross section of $\sigma = \lambda_{\text{dB}}^2/(2\pi)$, the unitarity-limited rate coefficient is [31]

$$K_2^{\text{unitarity}} = \sqrt{8\pi\hbar^4/(\mu^3 k_B T)}. \tag{5}$$

This highest achievable rate coefficient forms a fundamental limit that exists for every scattering process, however, it has only been investigated in many-atom systems so far.

We determine K_2 from the experimentally observed pair-loss rate γ_2 of our trapped atom pair [28,36]:

$$K_2 = \frac{\gamma_2}{\int d\mathbf{r}[n(\mathbf{r})]^2}, \tag{6}$$

where $n(\mathbf{r})$ is the normalized thermal density in the tweezer [28,32]. Since we model photoassociation in our system with two-timescale decay, there are two rate coefficients. Our experiments are performed close to the saturation intensity in order to compare to the corresponding unitarity-limited rate coefficient [Eq. (5)].

Figure 4 shows the photoassociation rate coefficients of fast and slow decaying populations in our two-atom experiments around the saturation intensity, and compares to the many-atom unitarity limit. The fast decay exceeds $K_2^{\text{unitarity}}$, whereas the rate coefficient for slow decay remains far below it. Recall that the many-atom unitarity-limited rate assumes that collisions happen randomly and depend on the average ensemble density. A plausible explanation for the fast decay exceeding the unitarity limit could be that peaked states have a higher probability of being at zero relative position than expected from the ensemble-averaged density. Note that in Fig. 4, a higher temperature does not imply a higher occupation of the tweezer states; in our experiments, atoms are prepared with similar starting temperature and different temperatures are achieved by adiabatically expanding the tweezer.

Photoassociation dynamics for three atoms.—As argued above, the two-timescale decay in the two-atom system is caused by pair correlation of the two atoms. Our setup allows the addition of a third atom to the tweezer, which we used to investigate photoassociation in a three-atom system and determine how the addition of an extra atom influences the dynamics. Figure 2(b) shows the evolution of the tweezer population starting with three atoms at 35 μK. We observe good agreement with a single decay rate above our detection limit of 1.6% and a reduced χ^2 test shows no improvement from the two-timescale model. The error bar of the point at 3.8 ms does overlap with the one-timescale fit (this is outside the frame of our logarithmic plot).

Additional measurements at photoassociation times greater than 4 ms give three-atom survival at our detection sensitivity limit, making them consistent with vanishing survival probability. The green triangles in Fig. 4, showing the single rate coefficient obtained with three atoms, are in good agreement with the many-atom unitarity-limited rate coefficient. Although we are reluctant to draw firm conclusions, these results suggest that the photoassociation dynamics take a substantial step toward the many-atom behavior when an additional atom is added to the tweezer.

Conclusions and outlook.—Photoassociation of single atoms is a promising path for creating precisely tailored single molecules not accessible through conventional chemistry. Understanding the photoassociation dynamics of single molecule formation is vital to the future controlled synthesis of more complex molecules. We showed the first measurement of the quantum dynamics of exactly two atoms undergoing photoassociation in an optical tweezer. We observed two rate coefficients which are caused by atom-pair correlations, as confirmed by numerical simulation of the two-atom system. In contrast, the photoassociation dynamics of three trapped atoms seem closer to that of many-atom ensembles. An interesting future work would be a more systematic investigation into how the many-atom dynamics emerge. Our results show that this state-dependent photoassociation could be used as a new tool for the production or detection of atom-pair correlations in future experiments.

We acknowledge useful discussions with and comments from Joachim Brand and Eite Tiesinga. This work was supported by the Marsden Fund Council from Government funding, administered by the Royal Society of New Zealand (Contract No. UOO1835). S. S. S. was supported by an Australian Research Council iscovery Early Career Researcher Award (DECRA), Project No. DE200100495. This research was undertaken with the assistance of resources and services from the National Computational Infrastructure (NCI), which is supported by the Australian Government.

*mikkel.andersen@otago.ac.nz

[1] A. Ashkin, J. M. Dziedzic, J. E. Bjorkholm, and S. Chu, Opt. Lett. **11**, 288 (1986).
[2] L. R. Liu, J. D. Hood, Y. Yu, J. T. Zhang, N. R. Hutzler, T. Rosenband, and K.-K. Ni, Science **360**, 900 (2018).
[3] L. R. Liu, J. D. Hood, Y. Yu, J. T. Zhang, K. Wang, Y. W. Lin, T. Rosenband, and K. K. Ni, Phys. Rev. X **9**, 021039 (2019).
[4] J. T. Zhang, Y. Yu, W. B. Cairncross, K. Wang, L. R. B. Picard, J. D. Hood, Y. W. Lin, J. M. Hutson, and K. K. Ni, Phys. Rev. Lett. **124**, 253401 (2020).
[5] R. P. Feynman, J. Microelectromech. Syst. **1**, 60 (1992).
[6] R. V. Krems, Phys. Chem. Chem. Phys. **10**, 4079 (2008).
[7] S. Ospelkaus, K.-K. Ni, D. Wang, M. H. G. de Miranda, B. Neyenhuis, G. Quéméner, P. S. Julienne, J. L. Bohn, D. S. Jin, and J. Ye, Science **327**, 853 (2010).
[8] P. Sompet, A. V. Carpentier, Y. H. Fung, M. McGovern, and M. F. Andersen, Phys. Rev. A **88**, 051401(R) (2013).
[9] T. Kinoshita, T. Wenger, and D. S. Weiss, Phys. Rev. Lett. **95**, 190406 (2005).
[10] C. P. Koch and R. Kosloff, Phys. Rev. Lett. **103**, 260401 (2009).
[11] T. Gasenzer, Phys. Rev. A **70**, 021603(R) (2004).
[12] M. Holland, J. Park, and R. Walser, Phys. Rev. Lett. **86**, 1915 (2001).
[13] P. Naidon and F. Masnou-Seeuws, Phys. Rev. A **73**, 043611 (2006).
[14] U. Schlöder, C. Silber, T. Deuschle, and C. Zimmermann, Phys. Rev. A **66**, 061403(R) (2002).
[15] C. McKenzie, J. Hecker Denschlag, H. Häffner, A. Browaeys, L. E. E. de Araujo, F. K. Fatemi, K. M. Jones, J. E. Simsarian, D. Cho, A. Simoni, E. Tiesinga, P. S. Julienne, K. Helmerson, P. D. Lett, S. L. Rolston, and W. D. Phillips, Phys. Rev. Lett. **88**, 120403 (2002).
[16] I. D. Prodan, M. Pichler, M. Junker, R. G. Hulet, and J. L. Bohn, Phys. Rev. Lett. **91**, 080402 (2003).
[17] S. Dutta, J. Lorenz, A. Altaf, D. S. Elliott, and Y. P. Chen, Phys. Rev. A **89**, 020702(R) (2014).
[18] R. Wester, S. D. Kraft, M. Mudrich, M. U. Staudt, J. Lange, N. Vanhaecke, O. Dulieu, and M. Weidemüller, Appl. Phys. B **79**, 993 (2004).
[19] K. M. Jones, E. Tiesinga, P. D. Lett, and P. S. Julienne, Rev. Mod. Phys. **78**, 483 (2006).
[20] T. Grünzweig, A. Hilliard, M. McGovern, and M. F. Andersen, Nat. Phys. **6**, 951 (2010).
[21] P. Sompet, S. S. Szigeti, E. Schwartz, A. S. Bradley, and M. F. Andersen, Nat. Commun. **10**, 1889 (2019).
[22] J. D. Miller, R. A. Cline, and D. J. Heinzen, Phys. Rev. Lett. **71**, 2204 (1993).
[23] R. A. Cline, J. D. Miller, and D. J. Heinzen, Phys. Rev. Lett. **73**, 632 (1994).
[24] T. Bergeman *et al.*, J. Phys. B **39**, S813 (2006).
[25] C. Degenhardt, T. Binnewies, G. Wilpers, U. Sterr, F. Riehle, C. Lisdat, and E. Tiemann, Phys. Rev. A **67**, 043408 (2003).
[26] L. A. Reynolds, E. Schwartz, U. Ebling, M. Weyland, J. Brand, and M. F. Andersen, Phys. Rev. Lett. **124**, 073401 (2020).
[27] C. P. Koch and M. Shapiro, Chem. Rev. **112**, 4928 (2012).
[28] See Supplemental Material at http://link.aps.org/supplemental/10.1103/PhysRevLett.126.083401, which includes Refs. [21,26,29–33], for details on the data analysis, control measurements, and numerical simulations.
[29] I. Hughes and T. Hase, *Measurements and Their Uncertainties: A Practical Guide to Modern Error Analysis* (Oxford University Press, New York, 2010).
[30] J. L. Bohn and P. S. Julienne, Phys. Rev. A **60**, 414 (1999).
[31] S. D. Kraft, M. Mudrich, M. U. Staudt, J. Lange, O. Dulieu, R. Wester, and M. Weidemüller, Phys. Rev. A **71**, 013417 (2005).
[32] R. Grimm, M. Weidemüller, and Y. B. Ovchinnikov, Adv. At. Mol. Opt. Phys. **42**, 95 (2000).

[33] M. R. Chernick, *Bootstrap Methods: A Guide for Practitioners and Researchers* (John Wiley & Sons, Inc., Hoboken, NJ, 2008).

[34] A. M. Kaufman, B. J. Lester, and C. A. Regal, Phys. Rev. X **2**, 041014 (2012).

[35] Computational requirements limited simulations to temperatures lower than the experiment [28].

[36] J. L. Roberts, N. R. Claussen, S. L. Cornish, and C. E. Wieman, Phys. Rev. Lett. **85**, 728 (2000).